ACS Chemical Neuroscience

UNIVERSITY OF BIRMINGHAM

Subscriber access provided by University of Birmingham

Letter

A Photoswitchable Inhibitor of the Human Serotonin Transporter

Bichu Cheng, Johannes Morstein, Lucy Kate Ladefoged, Jannick Bang Maesen, Birgit Schiøtt, Steffen Sinning, and Dirk Trauner

ACS Chem. Neurosci., **Just Accepted Manuscript** • DOI: 10.1021/acschemneuro.9b00521 • Publication Date (Web): 10 Apr 2020

A Photoswitchable Inhibitor of the Human Serotonin Transporter

Bichu Cheng[†,‡,&], Johannes Morstein[‡], Lucy Kate Ladefoged[#], Jannick Bang Maesen[§], Birgit Schiøtt[#], Steffen Sinning*[,§,&] and Dirk Trauner*[,‡]

[†]*School of Science, Harbin Institute of Technology (Shenzhen), Shenzhen 518055, China*

[‡]*Department of Chemistry, New York University, 100 Washington Square East, New York, New York 10003, United States*

[§]*Department of Forensic Medicine, Aarhus University, Palle Juul-Jensens Boulevard 99, 8200 Aarhus N, Denmark*

[#]*Department of Chemistry, Aarhus University, Langelandsgade 140, 8000 Aarhus C, Denmark*

[&]*These authors contributed equally*

ABSTRACT: The human serotonin transporter (hSERT) terminates serotonergic signaling through reuptake of neurotransmitter into presynaptic neurons and is a target for many antidepressant drugs. We describe here the development of a photoswitchable hSERT inhibitor, termed azo-escitalopram, that can be reversibly switched between *trans* and *cis* configurations using light of different wavelengths. The dark-adapted *trans* isomer, was found to be significantly less active than the *cis* isomer, formed upon irradiation.

Keywords: Photopharmacology, Serotonin, Transporter, Photochromic Ligand, Neurotransmitter

Serotonin (**1**) or 5-hydroxytryptamine (5-HT) is a monoamine neurotransmitter and plays a number of important roles in physiology and neurophysiology.[1,2] Most of the human body's serotonin is located in the enterochromaffin cells in the gastrointestinal tract, where it regulates intestinal movements. The remainder is synthesized from tryptophan in serotonergic neurons of the central nervous system, and is released into the synaptic cleft, where it activates serotonin receptors of the postsynaptic neurons. Serotonergic signaling influences neurological processes including sleep, mood, cognition, pain, hunger and aggression behaviours.[3] The serotonin transporter (SERT or 5-HTT) is a member of the neurotransmitter sodium symporter (NSS) family of transporters. It is responsible for the sodium- and chloride-dependent reuptake of serotonin from the synaptic cleft back to the presynaptic neuron, which terminates the serotonergic signaling and simultaneously enables the recycling of serotonin by the presynaptic neuron.[4]

Due to its importance in synaptic transmission and serotonin homeostasis, SERT has been subject to intense pharmacological studies, which gave rise to many clinically approved antidepressants.[5] Selective serotonin reuptake inhibitors (SSRIs), including citalopram (**2**), are used clinically to treat anxiety and depression (Fig. 1).[6,7] Citalopram (**2**) was developed by the pharmaceutical company Lundbeck and first marketed in 1989 in Denmark. It binds with high affinity and selectivity to SERT relative to other monoamine transporters.[8] Citalopram was originally used as a racemic mixture but Lundbeck later introduced the more potent (*S*)-enantiomer as escitalopram (**3**).

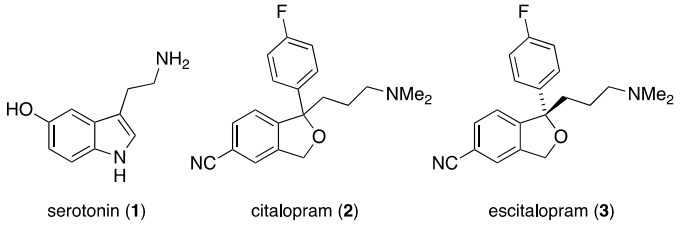

Figure 1. Chemical structures of serotonin, citalopram, and escitalopram.

Using *in silico* docking and experimental validation with a combination of citalopram analogs and hSERT mutants it was shown in 2010 that escitalopram binds to the same site as 5-HT, the S1 site.[9,10] Escitalopram was proposed to reside in an orientation wherein the protonated aliphatic tertiary amine forms a salt bridge to the conserved Asp98 in subsite A, the fluorophenyl group utilizes subsite B lined by Ala173, Asn177, and Thr439, whereas the cyanophenyl group engages subsite C lined by Phe335 and Phe341. This orientation was confirmed by X-ray crystallographic structure of human SERT bound to the antidepressant escitalopram in 2016.[11,12] Escitalopram locks SERT in an outward-open conformation by lodging in the central binding site, directly blocking serotonin binding and preventing the binding site from closing by protruding the cyanophenyl moiety through the aromatic lid normally occluding the substrate.[9–11] This implies that the cyano group will be most forgiving to chemical modifications because substituents would extend up through the extracellular vestibule towards a second allosteric site,[13] which is also supported by structure-

activity relationship studies on citalopram analogs,[14] in a similar fashion to what we have shown for substitutions on the 3-position of the tricyclic antidepressant imipramine.[15]

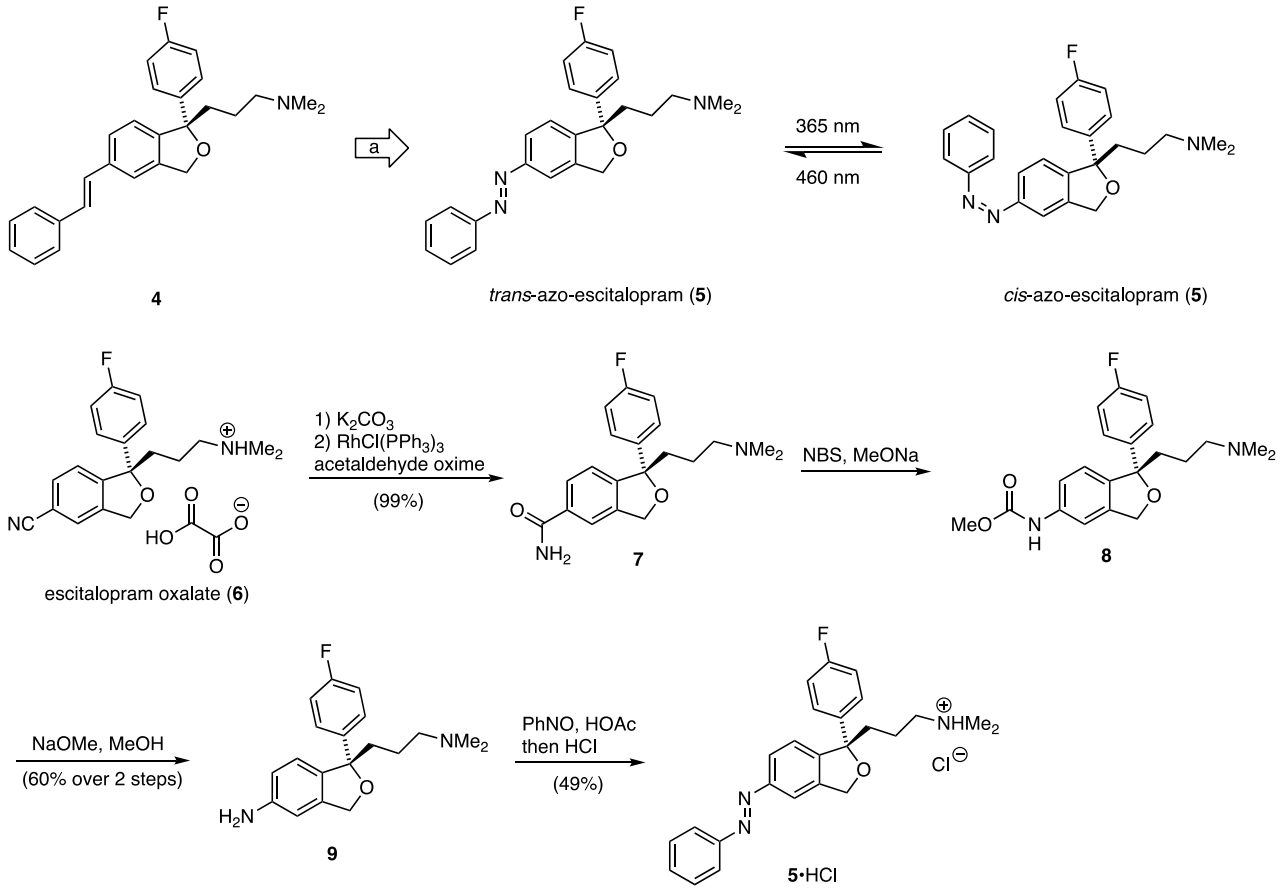

Scheme 1. Design and synthesis of azo-escitalopram (**5**).

In recent years, our group and others have developed a range of synthetic azobenzene photoswitches, either as freely diffusible photochromic ligands (PCLs), photoswitchable tethered ligands (PTLs), or photoswitchable orthogonal remotely tethered ligands (PORTLs), that can be used to optically control the function of many biological systems.[16–20] These include ion channels[21–23], G-protein coupled receptors (GPCRs)[24–26], enzymes[27,28], lipids[22,26,29], nuclear hormone receptors[30], and recently transporters[31–33]. We now describe the development of a photoswitchable azobenzene derivative of escitalopram that allows for the precise and reversible control of hSERT activity with light.

Extensive structure-activity studies at the 4- and 5-positions of the dihydroisobenzofuran moiety of escitalopram were conducted by the Newman group.[34] They found that replacement of the cyano group with a bulkier phenylvinyl (**4**) substituent retained most of the binding affinity with SERT (racemic K_i = 9.32 nM, (*S*)-enantiomer, K_i = 10.6 nM), and it showed higher binding affinity at SERT compared to its saturated phenylethyl analogue (racemic, K_i= 38.1 nM). Compound **4** is an azobenzene isostere ("azostere") which allows for straightforward design of an azobenzene analog which largely retains the structure of the parent compound. This well-precedented azologization approach[35] yields a version of escitalopram that can undergo photoisomerization. We hypothesized that the two photoisomers would exhibit marked structural differences, resulting in different potencies, which would enable the optical control of SERT activity.

We termed the azostere of the escitalopram derivate **4** "azo-escitalopram" (**5**). The synthesis of **5** began from commercially available escitalopram oxalate (**6**). Neutralization of **6** afforded the free amine, which underwent a rhodium-catalyzed nitrile hydration reaction to afford the primary amide **7**.[36] An NBS mediated Hofmann rearrangement and deprotection of the resulting carbamate **8** generated aniline **9**.[37] A Baeyer-Mills reaction of aniline **9** with nitrosobenzene then afforded the desired product **5**, which was isolated in its hydrochloride salt form (Scheme 1).

In its dark-adapted state, azo-escitalopram (**5**) exists in its thermally stable *trans* configuration with high absorption at 340 nm. It could be isomerized to its *cis*-form with

UV-A (λ = 365 nm) light. Isomerization from *cis* to *trans* could be achieved with blue light (λ = 460 nm). Photoisomerization could be repeated over many cycles without obvious fatigue. In its *cis* form, **5** remained stable in the dark (Scheme 2 B).

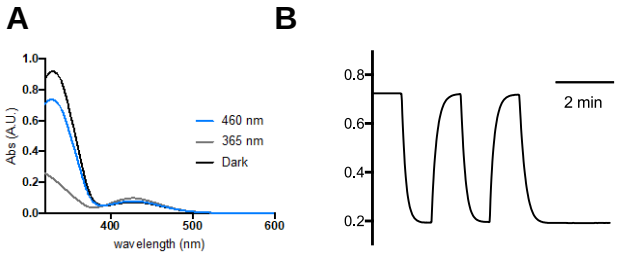

Scheme 2. Photoisomerization of azo-escitalopram (**5**) in 10% DMSO in PBS (50 μM). A) Absorption spectra of **5** in the dark-adapted, UV-A adapted, and blue-adapted state. B) Repeated cycles of *trans-cis* isomerization of **5** with 460 nm and 365 nm light.

With ample supplies of azo-escitalopram (**5**) in hand, we proceeded to test its action on the serotonin transporter. We performed uptake assays on HEK293MSR cells expressing hSERT to study the potency of **5** in inhibition of ^{3}H-5-HT uptake. A dilution series of **5** was prepared in the dark, mixed with ^{3}H-5-HT and then distributed to microwell plates where the compounds were either left in the dark or illuminated with 365 nm light from a handheld device for two seconds every minute in the time leading up to the experiment. Cells were first preincubated for 25 minutes with the inhibitor in either darkness or under illumination with 365 nm for two seconds every minute to achieve equilibrium. The uptake was initiated by addition of the inhibitor mixed with ^{3}H-5-HT and was allowed to proceed for 10 minutes in either darkness or under illumination with 365 nm for two seconds every minute. The uptake was terminated by aspiration and washing.

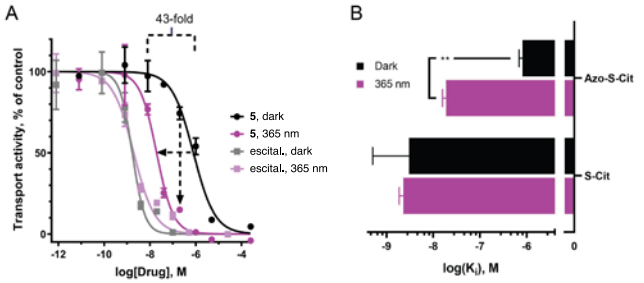

Figure 2. Azo-escitalopram (**5**) is a potent, photoswitchable inhibitor of the human serotonin transporter. (A) HEK293MSR cells were transiently transfected with hSERT in the pCDNA3 vector and exposed to the inhibitors either in the dark or illuminated at 365 nm for two seconds every minute prior to and during uptake of tritiated 5-HT. Shown is a representative example of normalized transport activity plotted as a function of drug concentration and fitted to a sigmoidal dose-response curve. Error bars represent standard error mean. (B) Mean K_i from three independent experiments show that the potency of the parent compound, escitalopram, is unaffected by irradiation at 365 nm whereas the inhibitory potency of **5** is significantly increased (P=0.0087, paired t-test) by photoswitching to the *cis* state by irradiation with light at 365 nm.

We found that the potency of escitalopram was, as expected, unaffected by darkness or light at 365 nm whereas the potency of **5** was low in the dark (*trans*-state) but increased 43-fold (p=0.0087, paired t-test) in the *cis*-state after illumination with 365 nm light. The potency of **5** in the *cis*-state was found to be 18.9 nM as compared to 819 nM in the *trans*-state. To confirmed that this increase in activity was not due to rapid degradation to a more potent derivative, we exposed **5** to glutathione (10 mM) for 1h in the presence and absence of light. The azobenzene was found to be stable under these conditions (Supporting Fig. 1)

In order to show that the photoswitchable inhibitor could be used to control the transport activity of hSERT in real time, we investigated the ability of **5** to photoswitch during an activity assay for the serotonin transporter (Figure 3). We initially equilibrated the transporter with *trans*-**5** at 460 nm for 20 minutes and then initiated uptake by addition of ^{3}H-5-HT. The inhibitor was maintained in the *trans* configuration for 8 minutes by brief illumination with light at 460 nm for two seconds every minute, after which the cells were exposed to different illumination regimes either by continued illumination at 460 nm for two seconds every minute to maintain the *trans* configuration or **5** was switched to the *cis* configuration by illumination at 365 nm for two seconds every minute for 22 minutes (figure 3A). We observed that 5-HT uptake was reduced significantly at 365 nm at three subsequent time points (Figure 3A) but also by comparing the normalized uptake rates in the linear phase (linear regression for incubation time 8-24 minutes) of the uptake assay in four independent experiments (Figure 3B).

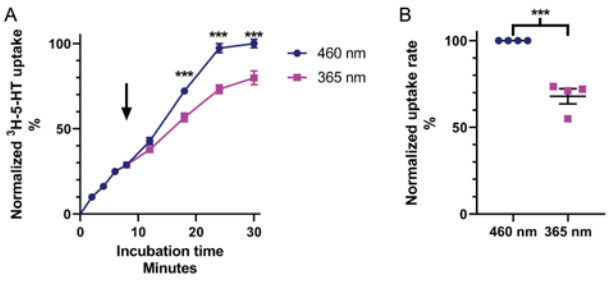

Figure 3. The transport activity of hSERT can be controlled in real time through different illumination regimes of azo-escitalopram (**5**). (A) HEK293MSR cells were transiently transfected with hSERT in the pCDNA3 vector and challenged with 200 nM **5** prior to and during uptake of tritiated 5-HT. Cells were briefly illuminated with 460 nm for two seconds every minute during 20 minutes of pre-incubation and for the first 8 minutes of the uptake assay. After 8 minutes of incubation with tritiated 5-HT half of the cells were then subjected to brief illumination with 365 nm for two seconds every minute (the shift in illumination regime

is marked by an arrow). Shown is the global fit of normalized data for four independent experiments where error bars on individual point represent SEM. Uptake at individual time points at different illumination regimes (12-30 minutes) were compared using the two-stage linear step-up procedure of Benjamini, Krieger and Yekutieli for paired t-test (p<0.001: ***).[38] (B) The uptake rates at 200 nM **5** was obtained from the slopes of the linear phase of the uptake assay at different illumination regimes (8-24 minutes in (A)) by linear regression analysis and then normalized to the uptake rates for cells challenged with 200 nM **5** illuminated with 460 nm. Comparison of the normalized uptake rates from four independent experiments exhibited highly statistically significant reduction (p<0.001, t-test) in uptake for hSERT exposed to *cis*-**5** (365 nm) as opposed to *trans*-**5** (460 nm).

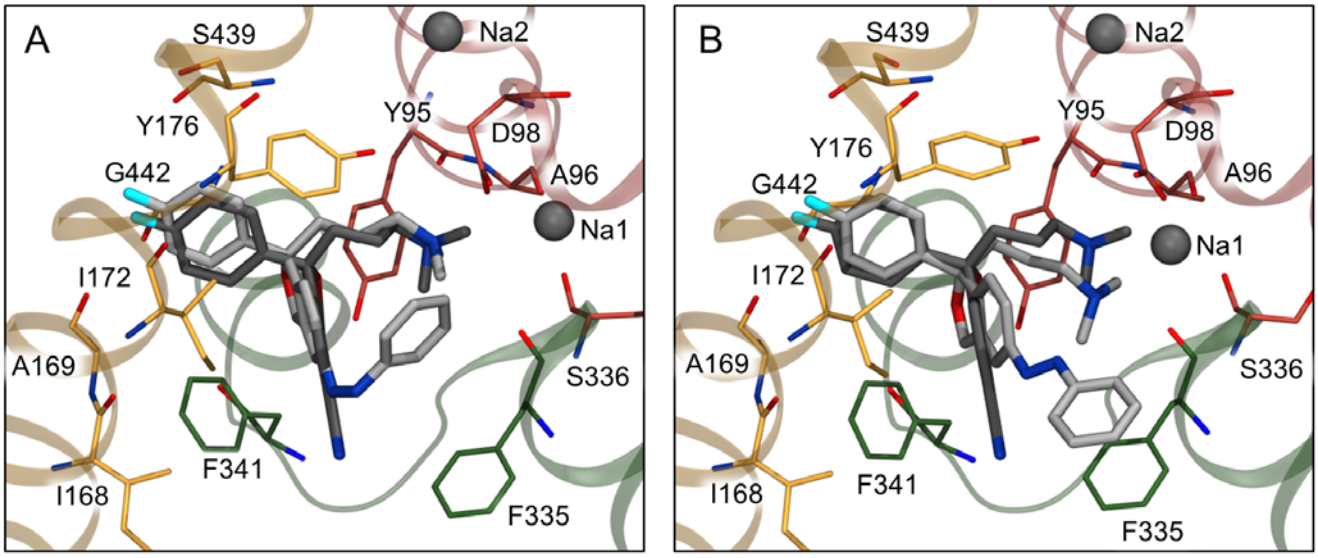

Figure 4. Induced fit docking of *cis*-**5** (left) and *trans*-**5** (right) demonstrates the molecular basis for hSERT selectivity for *cis*-**5**. (A) Out of a total of 100 docking poses for *cis*-**5** (light grey), 75 poses (*cis*-C2 cluster) assume a binding mode highly similar to the high-affinity parent inhibitor, escitalopram (dark grey). (B) Out of a total of 100 docking poses for *trans*-**5** (light grey), only 32 poses (*trans*-C12 cluster) assume a binding mode somewhat similar to the high-affinity parent inhibitor, escitalopram (dark grey), with notable disruption of the important salt bridge between the protonated amine of the inhibitor and the carboxylic acid side-chain of D98 as well as perturbations of the interactions between the inhibitor and the π-systems of Y95 and Y176.

Since the *trans* form of **5** sterically resembles the potent stilbene inhibitor **4**, it was unexpected, albeit welcome, that *cis*-**5** was more potent than *trans*-**5**. In order to better understand the *cis*-selectivity of **5**, we performed induced fit docking simulations (Figure 4). Docking of *cis*-**5** resulted in 100 poses which were clustered into 11 clusters, termed *cis*-C1–11 clusters (Supporting Table S1). Only one large cluster was identified: This *cis*-C2 cluster held 75 poses and contained the best scoring poses. Several elements in this cluster display the hallmarks of high-affinity inhibitors of hSERT identified earlier[10–12], most notably a salt bridge between the protonated amine of the ligand and Asp98 (55 of 75 poses), cation-π interaction between the protonated amine of the ligand and Tyr95 (73 of 75 poses) and a π-π interaction between the fluorophenyl of the ligand and Tyr176 (54 of 75 poses). Overall, *cis*-**5** exhibited most similarity with the binding of the parent inhibitor, escitalopram (Figure 4A), whereas *trans*-**5** produced a range of clusters, termed *trans*-C1–17 clusters, of which only two were of a significant size (27 and 32 out of 100 poses) (Supporting Table S1). For the *trans*-C1 cluster, the ligand is found more in the low-affinity allosteric S2 site rather than in S1[13,39,40], whereas the other major cluster (*trans*-C12) resembles the binding mode of the parent inhibitor, escitalopram (Figure 4B), albeit with some notable perturbations. For example, the important salt bridge between the protonated amine of the ligand and Asp98 is only found in less than one third of the *trans*-C12 poses (10 of 32 poses), the cation-π interaction between the protonated amine of the ligand and Tyr95 is found in only approximately half of the *trans*-C12 poses (17 of 32 poses) and a favourable π-π interaction between the fluorophenyl of the ligand and Tyr176 is found in less than half of the *trans*-C12 poses (15 of 32 poses). Overall, the significant similarity between *cis*-**5** binding and escitalopram binding as well of the retainment of well-established key protein-ligand interactions responsible for the high affinity of escitalopram[12] supports that *cis*-**5** should exhibit superior potency for inhibition of hSERT compared to *trans*-**5** as the experimental data also shows (Figure 2-3).

In conclusion, we have designed and synthesized azo-escitalopram (**5**) as the first photochromic inhibitor of hSERT and the first photopharmacological tool for serotonin biology at large. It can be reversibly switched be-

tween *trans* (low-affinity) and *cis* (high-affinity) configurations using light of different colors. We find that the *cis* configuration has nanomolar potency and is 43-fold more potent as an inhibitor than the *trans* configuration. Induced-fit docking calculations identify key protein-ligand interactions that are retained in *cis*-**5** and perturbed in *trans*-**5**. As such **5** could be a useful tool for the spatiotemporal regulation of serotonin in neural networks with the precision that light affords.

METHODS

Unless stated otherwise, all reactions were performed in oven-dried or heat gun dried glassware. Starting materials, solvents and reagents were obtained from commercial sources and used without further purification. Reactions were magnetically stirred and monitored by analytical thin-layer chromatography (TLC). TLC plates were visualized by exposure to ultraviolet light (UV, 254 nm). Flash column chromatography was performed employing silica gel (60 Å, 40-63 μm, Merck). Unless otherwise noted, yields refer to chromatographic and spectroscopic (1H and 13C NMR) pure materials. Proton and carbon nuclear magnetic resonance (^{1}H, ^{13}C NMR) spectra were recorded on a Bruker Avance III HD 400 MHz spectrometer with cryoprobe. Proton chemical shifts are expressed in parts per million (δ scale) and are calibrated using the residual undeuterated solvent as an internal reference (CDCl3: δ 7.26). Data for ^{1}H NMR spectra are reported as follows: chemical shift (δ ppm) (multiplicity, coupling constant (Hz), integration). Multiplicities are reported as follows: s = singlet, d = doublet, t = triplet, q = quartet, hept = heptet, appt = apparent, m = multiplet, br = broad or combinations thereof. Carbon chemical shifts are expressed in parts per million (δ scale) and are referenced to the carbon resonances of the solvent (CDCl3: δ 77.0). Infrared (IR) spectra were recorded on a Perkin Elmer Spectrum BX II (FTIR System) and reported in frequency of absorption (cm^{-1}). Mass spectroscopy (MS) experiments were performed on a Thermo Finnigan LTQ FT (ESI) instrument. Optical rotations were measured at 20 °C with a Krüss P8000-T polarimeter at the sodium-D line (589 nm), and the concentrations (c) are reported in units of g/100mL with the indicated solvent. UV/Vis spectra were recorded on a Varian Cary 60 Scan UV/Vis spectrometer equipped with an 18-cell holder using disposable UV cuvettes (1.5 – 3.0 mL chamber volume). Sample preparation and experiments were performed under red light conditions in a dark room. The solution was prepared from a 5 mM stock-solution in DMSO and diluted to 50 μM in PBS + 9% DMSO prior to the experiment. For illumination, a 12 x 5 mm 365 nm LED flashlight array (λ_{max} = 373 ± 17 nm) and a 21 x 5 mm 460 nm LED flashlight array (λ_{max} = 460 ± 10 nm) were used.

Glutathione reduction assay

5 (20 μM in 1% DMSO/PBS) was treated with PBS or reduced glutathione (10 mM) with and without prior irradiation at 365 nm for 4 minutes. After 1 hour, the samples were irradiated at 460 nm for 4 minutes to reach 460 nm adapted photostationary states in all samples for better direct comparison.

[^{3}H]-5-HT uptake assay

The uptake measurements were performed as previously described.[41] hSERT cDNA in the pcDNA3 vector (Invitrogen) was used to transiently transfect monolayer HEK-293 MSR cells (Invitrogen) in DMEM (BioWhitaker) supplemented with 10% FCS (Gibco Life Technologies), 100 U/ml penicillin, 100 μg/mL streptomycin (BioWhitaker) and 6 μg/mL of Geneticin (Invitrogen) at 95% humidity and 5% CO2 at 37 °C. In brief, two days before the uptake experiment, cells were detached from the culture flask with trypsin/EDTA (BioWhitaker), transfected with midiprep DNA-Lipofectamine 2000 (Life Technologies) or Ecotransfect (OZ Biosciences) complex and seeded into white tissue culture treated 96-well microtiter plates (Nunc). Immediately before the uptake experiment was initiated, medium was aspirated and cells were washed once with PBSCM (regular PBS buffer supplemented with calcium and magnesium: 137 mM NaCl, 27 mM KCl, 4.7 mM Na2HPO4, 1.2 mM KH2PO4, 0.1 mM CaCl2, 1 mM MgCl2, pH 7.4). Cells were preincubated with inhibitor for 20-25 minutes. Uptake was initiated by the addition of 40 μL of a dilution of the [3H]-5-HT mixed with inhibitor. Dilution series of inhibitors were done in the dark. During preincubation and incubation the inhibitors were either left in the dark or exposed to irradiation at 365 nm for 2 seconds every minute for the IC50 assay or exposed to irradiation at 365 nm or 460 nm for 2 seconds every minute for the realtime rescue of azo-escitalopram potency. Uptake was terminated after 10 minutes (IC50 assay) or at variable time points for the assay for realtime rescue of azo-escitalopram by aspiration and washing with PBSCM. 50 μL of Microscint 20 (Packard) was dispensed into each well resulting in cell lysis and release of accumulated radiolabelled substrate from the adherent cells allowing direct quantitation on a Packard Top-counter. Uptake data were fitted to sigmoidal dose-response curves by nonlinear regression analysis using the built-in tools in Prism8 (Graphpad).

Computational modelling

Protein preparation: The SERT structure was obtained from PDB entry 5I71[11] and prepared using the Protein Preparation Wizard[42] available in Maestro (Schrödinger Suite 2019, Schrödinger, LLC, New York, NY, 2019). This structure was chosen as SERT was co-crystallized with escitalopram in the central binding site. Residues with missing atoms were modelled using Prime and the protonation states of titratable residues were assessed by PROPKA,[43] both available in Maestro. The resulting protein model included two structural sodium ions and one structural water molecule coordinating one of the ions. A

cysteine bridge was modelled between Cys200 and Cys209, Glu508 was modelled in the protonated state, and His240 was modelled as the epsilon tautomer, while all other residues were modelled in their default states. *Ligand preparation*: The cis- and trans-azo-escitalopram molecules were drawn based on escitalopram from the PDB entry 5I71. The resulting bond orders and atomtypes were manually checked. Each molecule was first minimized in 5000 steps using a conjugant gradient method and then submitted to a conformational search using both the OPLS-2005 force field[44] and MacroModel available in Maestro. In the case of cis-azo-escitalopram, both calculations were performed with a dihedral restraint on the N=N bond (0±50° using a force constant of 100 kcal/mol) in order to retain the cis-isomer. All other settings were default. *Induced fit docking:* Both azo-escitalopram isomers were docked into SERT using the standard IFD protocol[45] available in Maestro. This protocal utilizes a three step docking protocol to achieve flexibility of both ligand and protein during docking. First, a softened docking is performed using 50% vdW interaction strength; secondly, the protein binding site sidechains are optimized in the context of the initially docked ligand; and thirdly, the ligand is re-docked into the now optimized binding site. The 200 best poses were allowed through the first docking step, while the 100 best poses were allowed through the final docking step. The first docking was performed in standard precision, while the last step was performed in extra precision. The resulting docking poses were clustered based on their conformation using the conformer cluster script available in Maestro. The number of clusters to use was determined for each ligand based on the minimum of the corresponding Kelley potential.

ASSOCIATED CONTENT

Supporting Information. Synthetic procedures and analytical data for new compounds; GSH reduction assay results; molecular docking results;

AUTHOR INFORMATION

Corresponding Author

stsi@forens.au.dk
dirktrauner@nyu.edu

Author Contributions

D.T. and S.S. conceived of this study. B.C., J.M., S.S., and D.T. designed experiments and wrote the paper with input from all authors. B.C. designed and performed chemical synthesis. B.C. and J.M. carried out photophysical characterization. J.M. performed the glutathione assay. S.S. and J.B.M. performed hSERT uptake assays. L.K.L. and B.L. performed molecular docking studies. All authors have participated in analysis of experiments and paper refinement.

ACKNOWLEDGMENT

J.M. thanks the German Academic Scholarship Foundation for a fellowship and New York University for a MacCracken fellowship and a Margaret and Herman Sokol fellowship. This work was supported by the National Institutes of Health (Grant R01NS108151-01). We are grateful to Simon Ravnkilde Sinning for designing and producing custom 3D-printed plastic polymer masks enabling controlled illumination of desired wells in microplates. We thank Grace Pan for assistance with the glutathione assay.

REFERENCES

(1) Berger, M.; Gray, J. A.; Roth, B. L. The Expanded Biology of Serotonin. *Annu. Rev. Med.* **2009**, *60* (1), 355–366. https://doi.org/10.1146/annurev.med.60.042307.110802.

(2) Göthert, M. Serotonin Discovery and Stepwise Disclosure of 5-HT Receptor Complexity over Four Decades. Part I. General Background and Discovery of Serotonin as a Basis for 5-HT Receptor Identification. *Pharmacol. Rep. PR* **2013**, *65* (4), 771–786.

(3) Nichols, D. E.; Nichols, C. D. Serotonin Receptors. *Chem. Rev.* **2008**, *108* (5), 1614–1641. https://doi.org/10.1021/cr078224o.

(4) Murphy, D. L.; Lesch, K.-P. Targeting the Murine Serotonin Transporter: Insights into Human Neurobiology. *Nat. Rev. Neurosci.* **2008**, *9* (2), 85–96. https://doi.org/10.1038/nrn2284.

(5) Artigas, F. Future Directions for Serotonin and Antidepressants. *ACS Chem. Neurosci.* **2013**, *4* (1), 5–8. https://doi.org/10.1021/cn3001125.

(6) Subbaiah, M. A. M. Triple Reuptake Inhibitors as Potential Therapeutics for Depression and Other Disorders: Design Paradigm and Developmental Challenges. *J. Med. Chem.* **2018**, *61* (6), 2133–2165. https://doi.org/10.1021/acs.jmedchem.6b01827.

(7) Zhong, H.; Haddjeri, N.; Sánchez, C. Escitalopram, an Antidepressant with an Allosteric Effect at the Serotonin Transporter--a Review of Current Understanding of Its Mechanism of Action. *Psychopharmacology (Berl.)* **2012**, *219* (1), 1–13. https://doi.org/10.1007/s00213-011-2463-5.

(8) Hyttel, J. Pharmacological Characterization of Selective Serotonin Reuptake Inhibitors (SSRIs). *Int. Clin. Psychopharmacol.* **1994**, *9 Suppl 1*, 19–26.

(9) Andersen, J.; Olsen, L.; Hansen, K. B.; Taboureau, O.; Jørgensen, F. S.; Jørgensen, A. M.; Bang-Andersen, B.; Egebjerg, J.; Strømgaard, K.; Kristensen, A. S. Mutational Mapping and Modeling of the Binding Site for (S)-Citalopram in the Human Serotonin Transporter. *J. Biol. Chem.* **2010**, *285* (3), 2051–2063. https://doi.org/10.1074/jbc.M109.072587.

(10) Koldsø, H.; Severinsen, K.; Tran, T. T.; Celik, L.; Jensen, H. H.; Wiborg, O.; Schiøtt, B.; Sinning, S. The Two Enantiomers of Citalopram Bind to the Human Serotonin Transporter in Reversed Orientations. *J. Am. Chem. Soc.* **2010**, *132* (4), 1311–1322. https://doi.org/10.1021/ja906923j.

(11) Coleman, J. A.; Green, E. M.; Gouaux, E. X-Ray Structures and Mechanism of the Human Serotonin Transporter. *Nature* **2016**, *532* (7599), 334–339. https://doi.org/10.1038/nature17629.

(12) Zeppelin, T.; Ladefoged, L. K.; Sinning, S.; Schiøtt, B. Substrate and Inhibitor Binding to the Serotonin Transporter: Insights from Computational, Crystallographic, and Functional Studies. *Neuropharmacology* **2019**, *161*,

107548. https://doi.org/10.1016/j.neuropharm.2019.02.030.
(13) Plenge, P.; Shi, L.; Beuming, T.; Te, J.; Newman, A. H.; Weinstein, H.; Gether, U.; Loland, C. J. Steric Hindrance Mutagenesis in the Conserved Extracellular Vestibule Impedes Allosteric Binding of Antidepressants to the Serotonin Transporter. *J. Biol. Chem.* **2012**, *287* (47), 39316–39326. https://doi.org/10.1074/jbc.M112.371765.
(14) Zhang, P.; Jørgensen, T. N.; Loland, C. J.; Newman, A. H. A Rhodamine-Labeled Citalopram Analogue as a High-Affinity Fluorescent Probe for the Serotonin Transporter. *Bioorg. Med. Chem. Lett.* **2013**, *23* (1), 323–326. https://doi.org/10.1016/j.bmcl.2012.10.089.
(15) Brinkø, A.; Larsen, M. T.; Koldsø, H.; Besenbacher, L.; Kolind, A.; Schiøtt, B.; Sinning, S.; Jensen, H. H. Synthesis and Inhibitory Evaluation of 3-Linked Imipramines for the Exploration of the S2 Site of the Human Serotonin Transporter. *Bioorg. Med. Chem.* **2016**, *24* (12), 2725–2738. https://doi.org/10.1016/j.bmc.2016.04.039.
(16) Hüll, K.; Morstein, J.; Trauner, D. In Vivo Photopharmacology. *Chem. Rev.* **2018**, *118* (21), 10710–10747. https://doi.org/10.1021/acs.chemrev.8b00037.
(17) Lerch, M. M.; Hansen, M. J.; van Dam, G. M.; Szymanski, W.; Feringa, B. L. Emerging Targets in Photopharmacology. *Angew. Chem. Int. Ed.* **2016**, *55* (37), 10978–10999. https://doi.org/10.1002/anie.201601931.
(18) Broichhagen, J.; Frank, J. A.; Trauner, D. A Roadmap to Success in Photopharmacology. *Acc. Chem. Res.* **2015**, *48* (7), 1947–1960. https://doi.org/10.1021/acs.accounts.5b00129.
(19) Beharry, A. A.; Woolley, G. A. Azobenzene Photoswitches for Biomolecules. *Chem. Soc. Rev.* **2011**, *40* (8), 4422–4437. https://doi.org/10.1039/C1CS15023E.
(20) Morstein, J.; Trauner, D. New Players in Phototherapy: Photopharmacology and Bio-Integrated Optoelectronics. *Curr. Opin. Chem. Biol.* **2019**, *50*, 145–151. https://doi.org/10.1016/j.cbpa.2019.03.013.
(21) Stawski, P.; Sumser, M.; Trauner, D. A Photochromic Agonist of AMPA Receptors. *Angew. Chem. Int. Ed.* **2012**, *51* (23), 5748–5751. https://doi.org/10.1002/anie.201109265.
(22) Frank, J. A.; Moroni, M.; Moshourab, R.; Sumser, M.; Lewin, G. R. Photoswitchable Fatty Acids Enable Optical Control of TRPV1. **2015**, *6*, 7118. https://doi.org/10.1038/ncomms8118.
(23) Damijonaitis, A.; Broichhagen, J.; Urushima, T.; Hull, K.; Nagpal, J.; Laprell, L.; Schonberger, M.; Woodmansee, D. H.; Rafiq, A.; Sumser, M. P.; Kummer, W.; Gottschalk, A.; Trauner, D. AzoCholine Enables Optical Control of Alpha 7 Nicotinic Acetylcholine Receptors in Neural Networks. *ACS Chem Neurosci* **2015**, *6* (5), 701–707. https://doi.org/10.1021/acschemneuro.5b00030.
(24) Schönberger, M.; Trauner, D. A Photochromic Agonist for μ-Opioid Receptors. *Angew. Chem. Int. Ed.* **2014**, *53* (12), 3264–3267. https://doi.org/10.1002/anie.201309633.
(25) Levitz, J.; Pantoja, C.; Gaub, B.; Janovjak, H.; Reiner, A.; Hoagland, A.; Schoppik, D.; Kane, B.; Stawski, P.; Schier, A. F.; Trauner, D.; Isacoff, E. Y. Optical Control of Metabotropic Glutamate Receptors. *Nat. Neurosci.* **2013**, *16* (4), 507–516. https://doi.org/10.1038/nn.3346.
(26) Morstein, J.; Hill, R. Z.; Novak, A. J. E.; Feng, S.; Norman, D. D.; Donthamsetti, P. C.; Frank, J. A.; Harayama, T.; Williams, B. M.; Parrill, A. L.; Tigyi, G. J.; Riezman, H.; Isacoff, E. Y.; Bautista, D. M.; Trauner, D. Optical Control of Sphingosine-1-Phosphate Formation and Function. *Nat. Chem. Biol.* **2019**, *15* (6), 623. https://doi.org/10.1038/s41589-019-0269-7.
(27) Tsai, Y.-H.; Essig, S.; James, J. R.; Lang, K.; Chin, J. W. Selective, Rapid and Optically Switchable Regulation of Protein Function in Live Mammalian Cells. *Nat. Chem.* **2015**, *7* (7), 554–561. https://doi.org/10.1038/nchem.2253.
(28) Broichhagen, J.; Jurastow, I.; Iwan, K.; Kummer, W.; Trauner, D. Optical Control of Acetylcholinesterase with a Tacrine Switch. *Angew Chem Int Ed Engl* **2014**, *53* (29), 7657–7660. https://doi.org/10.1002/anie.201403666.
(29) Frank, J. A.; Yushchenko, D. A.; Hodson, D. J.; Lipstein, N.; Nagpal, J.; Rutter, G. A.; Rhee, J.-S.; Gottschalk, A.; Brose, N.; Schultz, C.; Trauner, D. Photoswitchable Diacylglycerols Enable Optical Control of Protein Kinase C. *Nat Chem Biol* **2016**, *12* (9), 755–762. https://doi.org/10.1038/nchembio.2141.
(30) Morstein, J.; Trads, J. B.; Hinnah, K.; Willems, S.; Barber, D. M.; Trauner, M.; Merk, D.; Trauner, D. Optical Control of the Nuclear Bile Acid Receptor FXR with a Photohormone. *Chem. Sci.* **2020**, *11* (2), 429–434. https://doi.org/10.1039/C9SC02911G.
(31) Cheng, B.; Shchepakin, D.; Kavanaugh, M. P.; Trauner, D. Photoswitchable Inhibitor of a Glutamate Transporter. *ACS Chem. Neurosci.* **2017**, *8* (8), 1668–1672. https://doi.org/10.1021/acschemneuro.7b00072.
(32) Quandt, G.; Höfner, G.; Pabel, J.; Dine, J.; Eder, M.; Wanner, K. T. First Photoswitchable Neurotransmitter Transporter Inhibitor: Light-Induced Control of γ-Aminobutyric Acid Transporter 1 (GAT1) Activity in Mouse Brain. *J. Med. Chem.* **2014**, *57* (15), 6809–6821. https://doi.org/10.1021/jm5008566.
(33) Bonardi, F.; London, G.; Nouwen, N.; Feringa, B. L.; Driessen, A. J. M. Light-Induced Control of Protein Translocation by the SecYEG Complex. *Angew. Chem. Int. Ed.* **2010**, *49* (40), 7234–7238. https://doi.org/10.1002/anie.201002243.
(34) Zhang, P.; Cyriac, G.; Kopajtic, T.; Zhao, Y.; Javitch, J. A.; Katz, J. L.; Newman, A. H. Structure-Activity Relationships for a Novel Series of Citalopram (1-(3-(Dimethylamino)Propyl)-1-(4-Fluorophenyl)-1,3-Dihydroisobenzofuran-5-Carbonitrile) Analogues at Monoamine Transporters. *J. Med. Chem.* **2010**, *53* (16), 6112–6121. https://doi.org/10.1021/jm1005034.
(35) Morstein, J.; Awale, M.; Reymond, J.-L.; Trauner, D. Mapping the Azolog Space Enables the Optical Control of New Biological Targets. *ACS Cent. Sci.* **2019**, *5* (4), 607–618. https://doi.org/10.1021/acscentsci.8b00881.
(36) Lee, J.; Kim, M.; Chang, S.; Lee, H.-Y. Anhydrous Hydration of Nitriles to Amides Using Aldoximes as the Water Source. *Org. Lett.* **2009**, *11* (24), 5598–5601. https://doi.org/10.1021/ol902309z.
(37) Huang, X.; Keillor, J. W. Preparation of Methyl Carbamates via a Modified Hofmann Rearrangement. *Tetrahedron Lett.* **1997**, *38* (3), 313–316. https://doi.org/10.1016/S0040-4039(96)02341-6.
(38) Benjamini, Y.; Krieger, A. M.; Yekutieli, D. Adaptive Linear Step-up Procedures That Control the False Discovery Rate. *Biometrika* **2006**, *93* (3), 491–507. https://doi.org/10.1093/biomet/93.3.491.
(39) Chen, F.; Larsen, M. B.; Neubauer, H. A.; Sánchez, C.; Plenge, P.; Wiborg, O. Characterization of an Allosteric Citalopram-Binding Site at the Serotonin Transporter. *J. Neurochem.* **2005**, *92* (1), 21–28. https://doi.org/10.1111/j.1471-4159.2004.02835.x.
(40) Chen, F.; Larsen, M. B.; Sánchez, C.; Wiborg, O. The S-Enantiomer of R,S-Citalopram, Increases Inhibitor Binding to the Human Serotonin Transporter by an Allosteric

Mechanism. Comparison with Other Serotonin Transporter Inhibitors. *Eur. Neuropsychopharmacol. J. Eur. Coll. Neuropsychopharmacol.* **2005**, *15* (2), 193–198. https://doi.org/10.1016/j.euroneuro.2004.08.008.

(41) Sinning, S.; Musgaard, M.; Jensen, M.; Severinsen, K.; Celik, L.; Koldsoe, H.; Meyer, T.; Bols, M.; Jensen, H. H.; Schiott, B.; Wiborg, O. Binding and Orientation of Tricyclic Antidepressants within the Central Substrate Site of the Human Serotonin Transporter. *J. Biol. Chem.* **2009**, jbc.M109.045401. https://doi.org/10.1074/jbc.M109.045401.

(42) Madhavi Sastry, G.; Adzhigirey, M.; Day, T.; Annabhimoju, R.; Sherman, W. Protein and Ligand Preparation: Parameters, Protocols, and Influence on Virtual Screening Enrichments. *J. Comput. Aided Mol. Des.* **2013**, *27* (3), 221–234. https://doi.org/10.1007/s10822-013-9644-8.

(43) Olsson, M. H. M.; Søndergaard, C. R.; Rostkowski, M.; Jensen, J. H. PROPKA3: Consistent Treatment of Internal and Surface Residues in Empirical PKa Predictions. *J. Chem. Theory Comput.* **2011**, *7* (2), 525–537. https://doi.org/10.1021/ct100578z.

(44) Kaminski, G. A.; Friesner, R. A.; Tirado-Rives, J.; Jorgensen, W. L. Evaluation and Reparametrization of the OPLS-AA Force Field for Proteins via Comparison with Accurate Quantum Chemical Calculations on Peptides. *J. Phys. Chem. B* **2001**, *105* (28), 6474–6487. https://doi.org/10.1021/jp003919d.

(45) Sherman, W.; Day, T.; Jacobson, M. P.; Friesner, R. A.; Farid, R. Novel Procedure for Modeling Ligand/Receptor Induced Fit Effects. *J. Med. Chem.* **2006**, *49* (2), 534–553. https://doi.org/10.1021/jm050540c.

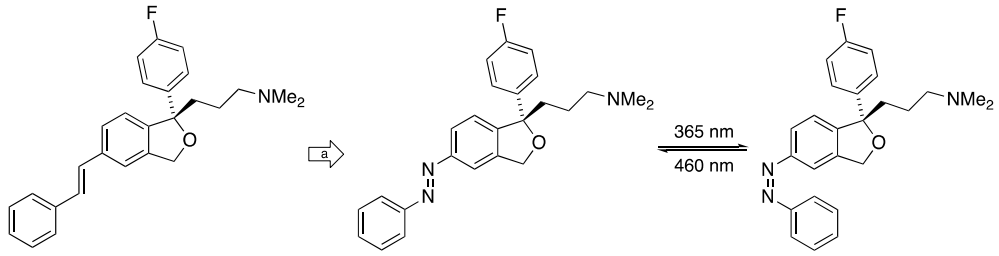

hSERT inhibitor *trans*-**azo-escitalopram** *cis*-**azo-escitalopram**